Design of Corrugated Waveguide Filters by Fourier-Transform Techniques

KIM A. WINICK, MEMBER, IEEE, AND JOSE E. ROMAN

Abstract—**A new, approximate, corrugated waveguide filter design method is developed for thin film optical waveguides. The method determines both the corrugation period and depth, measured along the guide's surface, given a specification of the filter's reflection coefficient. The design technique is based on a combined effective index approach and Fourier transform, inverse-scattering theory for one-dimensional, dispersionless, dielectric media. Use of the general technique is illustrated by the design of two corrugated waveguide filters. The design results are compared with those obtained using the first Born approximation, nonlinear renormalization, and the exact Gel'fand-Levitan-Marchenko method for two component inverse-scattering systems.**

I. INTRODUCTION

CORRUGATED thin film waveguides play a major role in lightwave devices [1]. Applications include distributed feedback lasing [2], bistable switching [3], phase matching in nonlinear materials [4]–[6], grating coupling [7], and optical filtering [8]–[15]. In many of these applications, the corrugation is periodic. In an aperiodically-corrugated thin film waveguide, however, the frequency-dependent coupling between waveguide modes can be used to produce a corrugated waveguide filter (CWF) which has a specified spectral response [11]. This response is often written as $r(\lambda)$, where r is the reflection coefficient of the filter and λ is wavelength. Techniques to determine the required corrugation, or equivalently the aperiodically-varying coupling coefficient, given $r(\lambda)$, have been previously proposed by Matsuhara *et al.* [16]–[17] and Song and Shin [18]. Matsuhara's approximate technique relies on the theory of linearly chirped gratings, while Song's method uses an exact quantum-mechanical inverse-scattering technique. In this paper, we develop a new design approach based on Fourier transform inverse-scattering methods [19]–[24] and the effective-index theory of waveguide modes [25].

The technique of Matsuhara and Hill starts with the well-known fact that the exchange of power between two contradirectional waveguide modes can be described by a pair of coupled-mode equations [25]. The unknowns in these equations are the spatial variation of the corrugation period and its depth measured along the guide. Their technique is based on three assumptions. First, at any wavelength λ, significant coupling between the two waveguide modes occurs only at the corrugation point $z(\lambda)$, where the Bragg condition is satisfied. Secondly, in regions centered about point $z(\lambda)$, the corrugation can be modeled as a constant depth, linearly chirped, grating. Thirdly, the reflection coefficient at wavelength λ can be computed as if the extent of the linearly chirped grating were infinite. Using these three approximations, a relationship is derived between the corrugation period and the corrugation depth at each point along the guide. Once the corrugation depth profile is given, the required corrugation period can be determined. As Matsuhara and Hill point out, their technique uses only the magnitude of the reflection coefficient, and thus it cannot be applied when the filter's phase response is specified. More importantly, the technique does not indicate how to choose the corrugation depth profile. Furthermore, Matsuhara and Hill give examples where an inappropriate choice yields a poor design.

The method of Song and Shin uses the Gelfand-Levitan-Marchenko (GLM) exact inverse-scattering technique, which was developed for quantum mechanics [26]. The goal of the quantum mechanical problem is to determine the Schrödinger wave equation potential function from the reflection coefficient. The Gelfand-Levitan-Marchenko (GLM) technique reformulates this inverse-scattering problem as a solution to an integral equation. For the one-dimensional Schrödinger equation, this integral equation reduces to a set of linear simultaneous equations. These equations can be solved numerically in a straightforward manner when the reflection coefficient is a rational function of wavelength. The GLM integral equation has also been applied to inverse scattering problems, where the scattering system is modeled as a pair of coupled-mode equations. Noting this fact, Song and Shin adopted the technique for CWF design. They showed that the GLM integral equation for the coupled-mode case also reduces to a set of linear simultaneous equations, and that these can be solved numerically for rational reflection coefficients. The technique is powerful but complex. In addition, it requires that the reflection coefficient be expressed as a rational polynomial function of wavelength.

The CWF-design method presented in this paper is a natural extension of the Fourier-transform inverse-scattering technique, developed by Delano [19] and Sossi [20]–[24], for one-dimensional, dispersionless, dielectric

Manuscript received November 27, 1989; revised June 8, 1990. This work was supported by the National Science Foundation Grant #ECS-8909802 and the Rackham Graduate School, University of Michigan, Ann Arbor.

The authors are with the Department of Electrical Engineering and Computer Science, University of Michigan, Ann Arbor, MI 48109.

IEEE Log Number 9039203.

media. This Fourier-transform technique has been successfully applied to dielectrics by Dobrowski *et al.* [27]–[29], Bovin and D. St. Germain [30], and Jaggard and Kim [31]. By establishing a connection between CWG filters and one-dimensional, stratified, dielectric media, we show that the Fourier-transform technique can be extended to CWF design.

The outline of this paper is as follows. In Section II optical propagation through a CWF is analyzed, along the lines of Basu and Ballantyne [32], using an effective index method. A two by two transfer matrix is derived for a small section of the guide, whose thickness measured perpendicular to the direction of propagation, is much less than the corrugation period. This matrix is shown to be identical to the corresponding matrix of a single-layer, homogeneous, dielectric slab provided: (1) the refractive index of the slab equals the local effective index of the guide, N_{eff}, and (2) the slab thickness is equal to the thickness of the guide section.

The value of N_{eff} is computed based on the local corrugation height of the guide section, the parameters of the guide, and the dispersion equation for a three material waveguide. Although the equivalent dielectric slab will exhibit some wavelength dispersion, this effect is small enough to be neglected. Thus, with the above provisions satisfied, the correspondence between propagation through one-dimensional, dispersionless, stratified, dielectric media and corrugated waveguides is established.

In Section III Fourier-transform inverse-scattering techniques are introduced for one-dimensional, dispersionless, dielectric media. Three different approximate solutions are derived, based upon the direct problem of determining the reflection coefficient $r(\lambda)$ given a one-dimensional refractive-index profile $n(z)$. Each of the solutions establishes a Fourier-transform relationship between $n(z)$ and a function of $r(\lambda)$.

Section IV combines the results of the previous two sections to yield an analytic procedure for the design of CWF. First, given a desired reflection coefficient $r(\lambda)$ the refractive index profile $n(z)$ is found using the Fourier-transform techniques of Section III. Next, the equivalent effective index profile $N_{\text{eff}}(z)$ is evaluated from $n(z)$ using the results of Section II. Finally, the waveguide corrugation is determined from $N_{\text{eff}}(z)$ by applying the waveguide dispersion equation.

In Section V two design examples are presented based on the above procedure, and good results are demonstrated. Fabrication issues are also briefly discussed. In Section VI our designs are compared to those obtained using the first Born approximation, a nonlinear renormalization technique, and the exact Gel'fand-Levitan-Marchenko approach for two-component scattering systems. These comparisons indicate that our technique is considerably more accurate than the first Born approximation, virtually identical to the nonlinear renormalization approach, and nearly as accurate as the more complex GLM method. Finally, Section VII contains a summary of our results.

II. The Effective Index Method

Consider the planar, thin film waveguide shown in Fig. 1. This is a three-layer dielectric guide, consisting of cover, film and substrate layers, having refractive indexes n_c, n_f, and n_s, respectively. The interface between the film and cover layers has a shallow surface corrugation, which is quasi-periodic. The film thickness of the guide is given by $h(z) = h_0 + \Delta h(z)$, where h_0 is the film thickness in the unperturbed regions. Light of free-space wavelength λ is confined to the film region by total internal reflection at the film-cover and film-substrate interfaces ($n_c < n_s < n_f$).

It is assumed that the film is sufficiently thin so that the guide only supports two TE-polarized, contradirectional, guided waves of the lowest order mode. These TE-polarized waves have an electric field component only along the y direction. Following a standard perturbation theory analysis, we write the electric field as

$$E_y(x, y, z) = E_{Fy}(x, y, z) + E_{By}(x, y, z) \quad (2.1)$$

where

$$E_{Fy}(x, y, z) = A(z)\, E(x) \exp\left[-i\beta(z)z\right] \quad (2.2)$$

$$E_{By}(x, y, z) = B(z)\, E(x) \exp\left[i\beta(z)z\right]. \quad (2.3)$$

The time dependence of the fields is assumed to be exp $[i\omega t]$. In (2.1)–(2.3), the subscripts F and B denote the forward-propagating (i.e., $+z$ direction) and backward-propagating (i.e., $-z$ direction) waves, respectively. $E(x)$ is the normalized mode profile supported by the guide in the unperturbed regions. $\beta(z)$ is the propagation constant, and it is given by the dispersion equation below [25]

$$V\left[1 - b\right]^{1/2} = \tan^{-1}\left[b/(1 - b)\right]^{1/2} + \tan^{-1}\left[(b + a)/(1 - b)\right]^{1/2} \quad (2.4)$$

where

$$V(z) = \frac{2\pi}{\lambda} h(z) \left[n_f^2 - n_s^2\right]^{1/2} \quad (2.5)$$

$$N_{\text{eff}}(z) = \beta(z)\, (2\pi/\lambda)^{-1} \quad (2.6)$$

$$b(z) = \left(N_{\text{eff}}^2(z) - n_s^2\right)/(n_f^2 - n_s^2) \quad (2.7)$$

$$a = (n_s^2 - n_c^2)/(n_f^2 - n_s^2). \quad (2.8)$$

$N_{\text{eff}}(z)$ is the local-effective index of the guide. We decompose the corrugated region of the film into N thin, parallel slabs of equal width $\Delta W_i = z_i - z_{i-1}$, with the geometry of the ith slab as indicated in Fig. 1. This slab is centered about the point $p_i = (z_{i-1} + z_i)/2$, and it is assumed to be sufficiently thin so that $h(z) \approx h(p_i) = h_i$, $\beta(z) \approx \beta(p_i) = \beta_i$, $A(z) \approx A(p_i) = A_i$, $B(z) \approx B(p_i) = B_i$, and $N_{\text{eff}}(z) \approx N_{\text{eff}}(z_i) = N_i$ for $z_{i-1} \le z \le z_i$. In the ith slab (2.2) and (2.3) can then be rewritten as

$$E_{Fy}(x, y, z) = A_i E(x) \exp\left[-i\beta_i(z - p_i)\right] \quad (2.9)$$

$$E_{By}(x, y, z) = B_i E(x) \exp\left[i\beta_i(z - p_i)\right]. \quad (2.10)$$

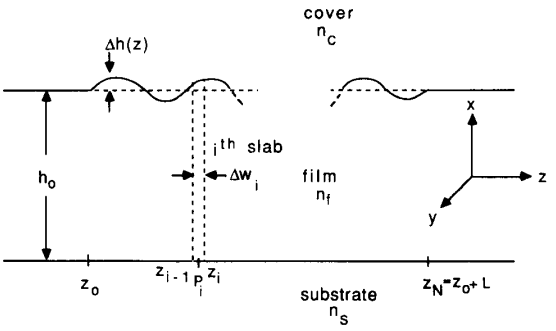

Fig. 1. Geometry of corrugated waveguide.

From Maxwell's equations it follows that

$$\nabla x E = -j\omega u H \tag{2.11}$$

where u is the permeability of free space and therefore

$$H_x(x, y, z) = H_{Fx}(x, y, z) + H_{Bx}(x, y, z) \tag{2.12}$$

where

$$H_{Fx}(x, y, z) = \frac{-\beta_i}{\omega u} E_{Fy}(x, y, z) \tag{2.13}$$

$$H_{Bx}(x, y, z) = \frac{\beta_i}{\omega u} E_{By}(x, y, z). \tag{2.14}$$

Let z_i^- and z_i^+ denote the values of z just to the left of and to the right of z_i, respectively. The electromagnetic boundary conditions require that E_y and H_x be continuous across interface between the $(i-1)$th and ith slabs. Therefore, it follows from (2.6), (2.13), and (2.14) that

$$\boldsymbol{V}_{i-1}\begin{bmatrix} E_{Fy}(x, y, z_{i-1}^-) \\ E_{By}(x, y, z_{i-1}^-) \end{bmatrix} = \boldsymbol{V}_i \begin{bmatrix} E_{Fy}(x, y, z_{i-1}^+) \\ E_{By}(x, y, z_{i-1}^+) \end{bmatrix} \tag{2.15}$$

where the matrix $\boldsymbol{V}_i$ is given by

$$\boldsymbol{V}_i = \begin{bmatrix} 1 & 1 \\ -N_i & N_i \end{bmatrix}. \tag{2.16}$$

It also follows immediately from (2.9) and (2.10) that propagation across the ith slab can be written as

$$\begin{bmatrix} E_{Fy}(x, y, z_{i-1}^+) \\ E_{By}(x, y, z_{i-1}^+) \end{bmatrix} = \boldsymbol{U}_i \begin{bmatrix} E_{Fy}(x, y, z_i^-) \\ E_{By}(x, y, z_i^-) \end{bmatrix} \tag{2.17}$$

where the matrix $\boldsymbol{U}_i$ is given by

$$\boldsymbol{U}_i = \begin{bmatrix} \exp\left[i \frac{2\pi}{\lambda} N_i \Delta w_i \right] & 0 \\ 0 & \exp\left[-i \frac{2\pi}{\lambda} N_i \Delta w_i \right] \end{bmatrix}. \tag{2.18}$$

Combining (2.15)–(2.18) yields

$$\begin{bmatrix} E_{Fy}(x, y, z_0^-) \\ E_{By}(x, y, z_0^-) \end{bmatrix} = \boldsymbol{V}_0^{-1} \left[\prod_{i=1}^{N} \boldsymbol{M}_i \right] \boldsymbol{V}_{N+1} \begin{bmatrix} E_{Fy}(x, y, z_N^+) \\ E_{By}(x, y, z_N^+) \end{bmatrix} \tag{2.19}$$

where

$$\boldsymbol{M}_i = \boldsymbol{V}_i \boldsymbol{U}_i \boldsymbol{V}_i^{-1} \tag{2.20}$$

Note that (2.19) relates the complex amplitude of the forward- and backward-propagating guided waves at the beginning of the corrugated section $z = z_0$ to the corresponding waves at the end $z = z_N = z_0 + L$. The CWF reflection and normalized transmission coefficients $r(\lambda)$ and $t(\lambda)$, respectively, are defined below for a guided wave incident at $z = z_0$.

$$r(\lambda) = \frac{E_{By}(x, y, z_0^-)}{E_{Fy}(x, y, z_0^-)} \quad \text{with } E_{By}(x, y, z_N^+) \text{ set to 0} \tag{2.21}$$

and

$$t(\lambda) = \frac{E_{Fy}(x, y, z_N^+) n(z_N^+)}{E_{Fy}(x, y, z_0^-) n(z_0^-)} \quad \text{with } E_{By}(x, y, z_N^+) \text{ set to 0.} \tag{2.22}$$

It can be shown that the above effective-index technique is valid for TE-mode propagation [33], and that it yields results equivalent to those obtained from a coupled-mode theory analysis [34]. The development given above can be paralleled for TM-modes, and (2.16), (2.18), (2.19), and (2.20) would be obtained unaltered. It is known, however, that this result is inconsistent with coupled-mode theory [25]. As noted by Verly *et al.* [35] this discrepancy occurs because the effective index method does not account for the boundary conditions at the corrugated surface–coverplate interface. For TE-modes this fact is not significant, since the E and H fields are always continuous across this interface. For TM-modes, however, there is a periodic discontinuity in E_x at the interface. This periodic discontinuity gives rise to an additional coupling term, which the effective-index analysis neglects. It is easy, however, to modify the effective-index method to include this effect [35], and thus extend our design technique to TM modes.

Consider now a dielectric of infinite extent in the x and y dimensions. Assume that the refractive index variation of the dielectric is only along the z-direction and that a normally incident plane wave strikes its front surface. It is clear that the analysis and the equations given above will remain valid, provided that: (1) $E(x)$ is replaced by a constant and (2) N_i is replaced by the refractive index of the ith slab at wavelength λ. Thus, TE-mode propagation through a CWF is equivalent to propagation

through a one-dimensional, stratified, dielectric media with refractive index $n(z) = N_{\text{eff}}(z)$.

$N_{\text{eff}}(z)$ is a function of wavelength λ, and therefore the refractive index in the equivalent dielectric medium must exhibit dispersion. In most cases, however, the dispersion can be neglected over the filter band of interest. This fact is shown below by bounding the dispersive term in the $\boldsymbol{U}_i$ and $\boldsymbol{V}_i$ matrices. We start with the following two expressions, which are derived in the Appendix.

$$\frac{\Delta_\lambda N_{\text{eff}}(z)}{N_{\text{eff}}(z)} = -\frac{h(z)}{h_{\text{eff}}(z)} \frac{\left(n_f^2 - N_{\text{eff}}^2(z)\right)}{N_{\text{eff}}^2(z)} \frac{\Delta\lambda}{\lambda} \tag{2.23}$$

$$\frac{\Delta_h N_{\text{eff}}(z)}{N_{\text{eff}}(z)} = \frac{h(z)}{h_{\text{eff}}(z)} \frac{\left(n_f^2 - N_{\text{eff}}^2(z)\right)}{N_{\text{eff}}^2(z)} \frac{\Delta h}{h(z)}. \tag{2.24}$$

$\Delta_\lambda N_{\text{eff}}(z)$ and $\Delta_h N_{\text{eff}}(z)$ are the changes in effective index due to wavelength, and film thickness changes $\Delta\lambda$ and Δh, respectively. $h_{\text{eff}}(z)$ is the effective film height and is given by [25]

$$h_{\text{eff}}(z) = \frac{\left(V + b^{-1/2}(z) + \left(a + b(z)\right)^{-1/2}\right)}{\frac{2\pi}{\lambda}\left[n_f^2 - n_s^2\right]^{1/2}}. \tag{2.25}$$

$h_{\text{eff}}(z)$ equals the actual film height $h(z)$ plus the $1/e$ amplitude penetration depths of the guided mode into the substrate and coverplate regions. Typically, $h_{\text{eff}}(z) < 2h(z)$.

Consider first the $\boldsymbol{V}_i$ matrix. In general, $\Delta\lambda/\lambda$ is quite small compared to the maximum values of $\Delta h/h(z)$, which are typically a few percent [8]. For instance, if the desired filter has a reflection bandwidth of 10 Å and the band center is at a wavelength of 5000 Å, then $\Delta\lambda/\lambda \approx 10^{-3}$. It therefore follows from (2.23) and (2.24) that $\Delta_\lambda N_{\text{eff}}(z) \ll \Delta_h N_{\text{eff}}(z)$. Thus, the effect of $\Delta_\lambda N_{\text{eff}}(z)$ can usually be neglected in the $\boldsymbol{V}_i$ matrices.

Next, we will examine the $\boldsymbol{U}_i$ matrix. Using the fact that $h(z) < h_{\text{eff}}(z)$, (2.23) can be rewritten as

$$\left|\frac{\Delta_\lambda N_{\text{eff}}(z)/N_{\text{eff}}(z)}{\Delta\lambda/\lambda}\right| < \frac{\left(n_f^2 - N_{\text{eff}}^2\right)}{N_{\text{eff}}^2(z)} < \frac{\left(n_f^2 - n_s^2\right)}{n_s^2}. \tag{2.26}$$

Consider now the phase factor $(2\pi/\lambda)N_i\Delta W_i$ in the $\boldsymbol{U}_i$ matrix. The change of this factor, due to a change $\Delta\lambda$ in wavelength, is given by

$$-\frac{2\pi}{\lambda^2} N_i(\Delta W_i)(\Delta\lambda) + \frac{2\pi}{\lambda}(\Delta_\lambda N_i)(\Delta W_i). \tag{2.27}$$

The first and second terms in this expression represent the nondispersive and the wavelength dispersive phase contributions, respectively. In practice, the film index, n_f, is often close in value to the substrate index n_s. Thus from (2.26), it follows that the wavelength dispersive term in $\boldsymbol{U}_i$ is usually small compared to the nondispersive contribution.

III. Inverse Scattering Using the Fourier Transform

Consider an isotropic dielectric slab of infinite extent in the x and y dimensions. Along the z direction, the slab is bounded by the $z = 0$ and $z = L$ planes. The refractive index, $n(z)$, is constant in the half spaces $z \le 0$ and $z \ge L$, continuous everywhere, and varies only as a function of z. A plane wave traveling in the $+z$ direction is normally incident upon the slab interface $z = 0$. The total electric field $E_y(x, y, z)$ can be written as

$$E_y(x, y, z) = E_{Fy}(x, y, z) + E_{By}(x, y, z) \tag{3.1}$$

where the electric fields $E_{Fy}(x, y, z)$ and $E_{By}(x, y, z)$ correspond to plane waves propagating in the $+z$ and $-z$ directions, respectively. The reflection and normalized transmission coefficients r and t, for a forward-propagating wave incident at z, are defined by

$$r(\lambda, z) = \frac{E_{By}(x, y, z)}{E_{Fy}(x, y, z)} \tag{3.2}$$

and

$$t(\lambda, z) = \frac{E_{Fy}(x, y, L)}{E_{Fy}(x, y, z)} \frac{n(L)}{n(z)}. \tag{3.3}$$

Note that $R(\lambda) = |r(\lambda, 0)|^2$ is the fraction of incident power reflected at the $z = 0$ boundary. Similarly, $T(\lambda) = |t(\lambda, 0)|^2 = 1 - R(\lambda)$ equals the fraction of incident power transmitted through the $z = L$ surface.

The goal of one-dimensional inverse scattering is to obtain $n(z)$ given $r(\lambda, 0)$ data. Many techniques are available to perform this task, each having a different degree of accuracy and complexity. We have restricted our analysis to Fourier based methods since they are (1) simple to understand, (2) very easy to implement, (3) numerically stable, and (4) yield reasonably accurate results. The exact GLM technique, which is considerably more complex, is discussed in Section VI. The following Fourier design relationships will be used to design corrugated waveguide filters.

$$r(\lambda, 0) \approx \int_0^{s_L} \frac{\boldsymbol{n}'(s)}{2\boldsymbol{n}(s)} e^{-iks}\, ds \quad \text{provided } |r(\lambda, 0)| \ll 1 \tag{3.4}$$

$$\left[\frac{1}{2}\left(\frac{1}{T(\lambda)} - T(\lambda)\right)\right]^{1/2} \approx \left|\int_0^{s_L} \frac{\boldsymbol{n}'(s)}{2\boldsymbol{n}(s)} e^{-iks}\, ds\right| \tag{3.5}$$

$$\tanh^{-1}\left[r(\lambda, 0)\right] \approx \int_0^{s_L} \frac{\boldsymbol{n}'(s)}{2\boldsymbol{n}(s)} e^{-iks}\, ds \tag{3.6}$$

where $k = 2\pi/\lambda$, the prime denotes a derivative, and $\boldsymbol{n}(s)$ equals the refractive index, given as a function of twice the optical path length s; s and s_L are given below:

$$s(z) = 2\int_0^z n(u)\, du \tag{3.7}$$

$$s_L = 2\int_0^L n(u)\, du. \tag{3.8}$$

Observe that (3.7) can also be written as

$$z = \int_0^s \frac{1}{2\boldsymbol{n}(s)}\, ds. \tag{3.9}$$

Defining $f(k)$ by either

$$f(k) = r(\lambda, 0) \qquad \text{for } |r(\lambda, 0)| \ll 1 \tag{3.10}$$

or

$$f(k) = \left[\frac{1}{2}\left(\frac{1}{T(k)} - T(k)\right)\right]^{1/2} \exp\left[i\phi(k)\right] \tag{3.11}$$

or

$$f(k) = \tanh^{-1}\left(r(\lambda, 0)\right) \tag{3.12}$$

and letting $L \to \infty$, (3.4)–(3.6) can be rewritten as

$$f(k) \approx \int_{-\infty}^{\infty} \frac{\boldsymbol{n}'(s)}{2\boldsymbol{n}(s)}\, e^{-iks}\, ds. \tag{3.13}$$

Inversion of this Fourier transform yields

$$\frac{\boldsymbol{n}'(s)}{2\boldsymbol{n}(s)} \approx \frac{1}{2\pi} \int_{-\infty}^{\infty} f(k)\, e^{iks}\, ds \tag{3.14}$$

where $f(-k) \triangleq f^*(k)$, $k \geq 0$.

Equation (3.14) is the approximate solution to the one-dimensional, inverse scattering problem for dispersionless, dielectric media. Given $r(\lambda, 0)$ or $T(k)$, (3.14) together with either (3.10), (3.11), or (3.12) can be used to determine $\boldsymbol{n}(s)$. The refractive index profile is then computed, as a function of z, from (3.9). The Fourier-transform relationship between $n(z)$ and $f(k)$, expressed by (3.11) and (3.14), will be applied in Section IV to design CWG filters. For comparison purposes designs based on (3.10) and (3.12) will also be examined. Equations (3.11) and (3.12) will be found to yield designs of nearly equal accuracy, while (3.10) will produce a significantly inferior result. Equation (3.4) is the well-known first Born approximation. In the literature [31], the design technique based on (3.6) is sometimes referred to as nonlinear renormalization.

Equations (3.5) and (3.6) were first derived by Sossi [20] and Greenewalt *et al.* [36], respectively. The derivation of (3.4) and (3.6) follows directly from the Ricatti differential equation for $r(\lambda, s)$ [37]. (Below we omit the explicit dependence of r on λ for notational simplicity.)

$$r'(s) = \frac{\boldsymbol{n}'(s)}{2\boldsymbol{n}(s)}\left[1 - r^2(s)\right] + ikr(s). \tag{3.15}$$

For low reflectivity (i.e., $|r(0)|^2 \ll 1$), the $r^2(s)$ term can be neglected in (3.15), and direct integration then yields (3.4). At higher reflectivities, we observe [31]

$$\tanh^{-1}\left[r(s)\right] \approx \frac{r(s)}{1 - r^2(s)}. \tag{3.16}$$

Equation (3.16) is recognized as the first term in a Taylor series expansion of $r(s)$ about the complex point $r(s) = 0$, since

$$\frac{d}{dz}\tanh^{-1}(z) = \frac{1}{1 - z^2} \qquad \text{for } z \text{ a complex number} \tag{3.17}$$

and $\tanh^{-1}(0) = 0$. It also follows from (3.17) that

$$\frac{d}{ds}\tanh^{-1}\left(r(s)\right) = \frac{r'(s)}{1 - r^2(s)}. \tag{3.18}$$

Combining (3.15), (3.16), and (3.18) yields

$$\frac{d}{ds}\tanh^{-1}\left(r(s)\right) \approx \frac{\boldsymbol{n}'(s)}{2\boldsymbol{n}(s)} + ik\tanh^{-1}\left[r(s)\right]. \tag{3.19}$$

Direct integration of (3.19) now produces (3.6). The derivation of (3.5) can be found in [20], [21].

IV. CWG Filter Design

The results derived above will now be applied to the design of CWG filters. In view of the conclusions of Section II (3.13) and (3.7) become

$$f(k) \approx \int_{-\infty}^{\infty} \frac{\boldsymbol{N}'_{\text{eff}}(s)}{2\boldsymbol{N}_{\text{eff}}(s)}\, e^{-iks}\, ds \tag{4.1}$$

$$s(z) = 2\int_0^z \boldsymbol{N}_{\text{eff}}(u)\, du. \tag{4.2}$$

We now write $\boldsymbol{N}_{\text{eff}}(s)$ in the following form:

$$\boldsymbol{N}_{\text{eff}}(s) = N_0 + \Delta\boldsymbol{N}_{\text{eff}}(s) \tag{4.3}$$

where we assume that

$$\left|\Delta\boldsymbol{N}_{\text{eff}}(s)\right| \ll N_0. \tag{4.4}$$

This assumption is consistent with a requirement that the depth of the surface corrugation not exceed a small fraction of the waveguide height. In most cases of practical interest, the desired reflection coefficient $r(\lambda, 0)$ is only nonzero over a small wavelength interval. For example, consider a sharp cut-off reflection filter centered at 5005 Å with a bandwidth of 10 Å

$$r(\lambda) = \begin{cases} 1 & \text{for } 5000 \text{ Å} \leq \lambda \leq 5010 \text{ Å} \\ 0 & \text{elsewhere.} \end{cases}$$

In these cases, it follows from (4.1) that $d(\Delta\boldsymbol{N}_{\text{eff}}(s))/ds$ is the Fourier transform of a narrowband function $f(k)$, and therefore $\Delta\boldsymbol{N}_{\text{eff}}(s)$ is quasi-sinusoidal. Thus we can write

$$\Delta\boldsymbol{N}_{\text{eff}}(s) = \delta\boldsymbol{N}_{\text{eff}}(s)\cos\left[k_0 s + \boldsymbol{\theta}(s)\right] \tag{4.5}$$

where $\pi/(k_0^2 N_0)$ is the nominal period of the surface grating. Note that this nominal period satisfies the Bragg condition for light of wavelength $2\pi/\lambda_0$. Combining (4.1), (4.3), and (4.4) yields

$$f(k) \approx \frac{ik}{2N_0}\int_{-\infty}^{\infty} \delta\boldsymbol{N}_{\text{eff}}(s)\cos\left(k_0 s + \boldsymbol{\theta}(s)\right) e^{-iks}\, ds \tag{4.6}$$

$$= \frac{ik}{4N_0} \int_{-\infty}^{\infty} \delta N_{\text{eff}}(s)\, e^{i\theta(s)}\, e^{-i(k-k_0)s}\, ds + \frac{ik}{4N_0} \int_{-\infty}^{\infty} \delta N_{\text{eff}}(s) - e^{i\theta(s)}\, e^{-i(k+k_0)s}\, ds. \tag{4.7}$$

The second integral in (4.7) contains the complex exponential $e^{-i(k+k_0)s}$ which varies very rapidly as a function of s, and therefore this integral is nearly zero. Hence, (4.7) can be written as

$$f(\Delta k) \approx \frac{ik}{4N_0} \int_{-\infty}^{\infty} \delta N_{\text{eff}}(s)\, e^{i\theta(s)}\, e^{-i\Delta k s}\, ds \tag{4.8}$$

where

$$\Delta k = k - k_0. \tag{4.9}$$

Inversion of (4.8) yields

$$\delta N_{\text{eff}}(s)\, e^{i\theta(s)} = \frac{-i2N_0}{\pi} \int_{-\infty}^{\infty} \frac{f(\Delta k)}{k_0 + \Delta k}\, e^{i\Delta k s}\, d(\Delta k). \tag{4.10}$$

It follows from (4.2) and (4.4) that

$$s \approx 2N_0 z. \tag{4.11}$$

Combining (4.10) and (4.11) gives our final result

$$\delta N_{\text{eff}}(z)\, e^{i\theta(z)} \approx \frac{-i2N_0}{\pi} \int_{-\infty}^{\infty} \frac{f(\Delta k)}{k_0 + \Delta k}\, e^{i(\Delta k)2N_0 z}\, d(\Delta k) \tag{4.12}$$

$$\approx \frac{-i2N_0}{\pi k_0} \int_{-\infty}^{\infty} f(\Delta k)\, e^{i(\Delta k)2N_0 z}\, d(\Delta k). \tag{4.13}$$

Once N_0 and k_0 are specified, $\Delta N_{\text{eff}}(z)$ is easily computed from either (4.12) or (4.13). We also note that these computations are numerically stable. Normally k_0 will be choosen to lie near the center of the reflection coefficient's wavelength band. This choice will produce a θ, which is a slowly varying function of z.

The $\Delta N_{\text{eff}}((z)$ given by (4.12) can be physically realized by corrugating the waveguide height h. The relationship between the local height corrugation $\Delta h(z)$ and $\Delta N_{\text{eff}}(z)$ is given by (2.24). With $|\Delta N_{\text{eff}}(z)| << N_0$, this equation becomes

$$\Delta h(z) \approx \frac{N_0 h_{\text{eff}}(0)}{n_f^2 - N_0^2}\, \Delta N_{\text{eff}}(z). \tag{4.14}$$

Equations (4.13) and (4.14), together with the $f(k)$'s specified by (3.10), (3.11), or (3.12), constitute the CWG filter design solution.

Finally, we note that an almost-periodic square wave can be represented as the sum of an infinite number of quasi-sinusoidal terms. At most a single quasi-sinusoidal term in this representation will contribute to the integral of (4.1). The remaining terms will make negligible contributions since they will not be phase matched to the complex exponential e^{-iks} appearing in the integrand. Therefore, the quasi-sinusoidal $\Delta N_{\text{eff}}(z)$ can be replaced by a quasi-periodic square wave without affecting $r(\lambda, 0)$. Each cycle of this square wave will have the same period as the corresponding sinusoid, but an amplitude which is smaller by a factor of $\pi/4$. This $\pi/4$ factor is the reciprocal of the first coefficient in the Fourier series expansion of a square wave.

V. Design Examples

In this section, two CWG filter design examples are presented. The designs are performed using Sossi's Fourier transform technique as described by (3.11) and (4.13). The design process proceeds in five steps. First, the desired filter reflectance $R(\lambda)$ is specified. Second, $\Delta N_{\text{eff}}(z)$ is computed using (4.13) and (3.11), with $\phi(k)$ set to zero, and the required integration performed numerically. Third, the period $\Lambda(z)$ of each cycle of the resulting quasi-sinusoidal effective index profile is computed as

$$\Lambda(z) = \frac{2\pi}{2k_0 N_0 + \dfrac{d\theta(z)}{dz}}. \tag{5.1}$$

Fourth, the filter length is truncated at the point where $|\delta N_{\text{eff}}(z)|$ falls below approximately 10% of its maximum value. Fifth, the quasi-sinusoidal profile is replaced by a quasi-periodic square wave profile. Each cycle of this square wave has the same period as the corresponding sinusoid, but an amplitude which is smaller by a factor of $\pi/4$. Finally, the reflectance of the resulting filter is determined using the matrix-based effective index method described in Section II.

Two filters, one "linear" and one "parabolic," were designed using the technique described above. Good results were obtained in both cases as indicated by Figs. 2 and 3. The design computations were performed in less than one minute on a MACIIx personal computer. For the "linear" filter λ_0 and N_0 were chosen to be 0.5005 μm and 1.5, respectively. Similarly, for the parabolic design $\lambda_0 = 0.5000$ μm and $N_0 = 1.5$. The amplitude $\delta N_{\text{eff}}(z)$ and the period $\Lambda(z)$ for the linear filter design are plotted in Figs. 4 and 5. Figs. 6 and 7 are the equivalent plots for the parabolic design. A negative value for $\delta N_{\text{eff}}(z)$ in Fig. 6 indicates a π phase shift in the sinusoidal grating corrugation. Note that the period is constant in Fig. 7. This constant periodicity follows directly from (4.13), since $\theta(z)$ will be either 0 or π when $f(k)$ is symmetrical about k_0.

Fabrication of nonperiodic corrugated waveguide filters is clearly a difficult task given the feature sizes involved. Below, we present some preliminary thoughts on the process. Two parameters define the filter, the effective index "variation" $\delta N_{\text{eff}}(z)$ and the period $\Lambda(z)$. A careful examination of the analysis presented in Section II of this

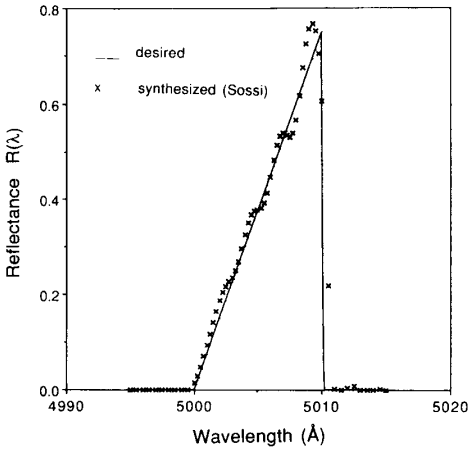

Fig. 2. Linear corrugated waveguide filter.

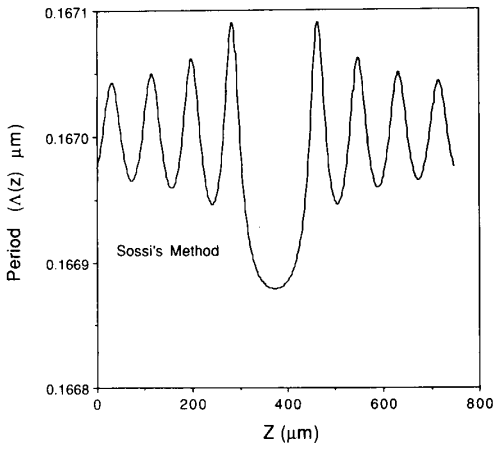

Fig. 5. Effective index period profile for the linear CWG filter.

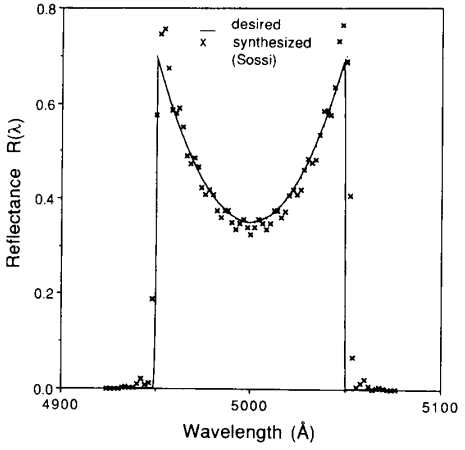

Fig. 3. Parabolic corrugated waveguide filter.

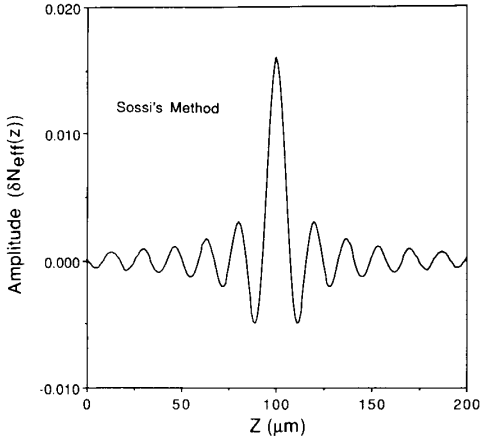

Fig. 6. Effective index period profile for the parabolic CWG filter.

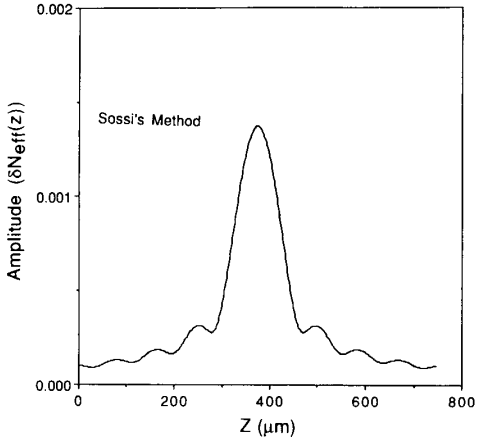

Fig. 4. Effective index amplitude profile for the linear CWG filter.

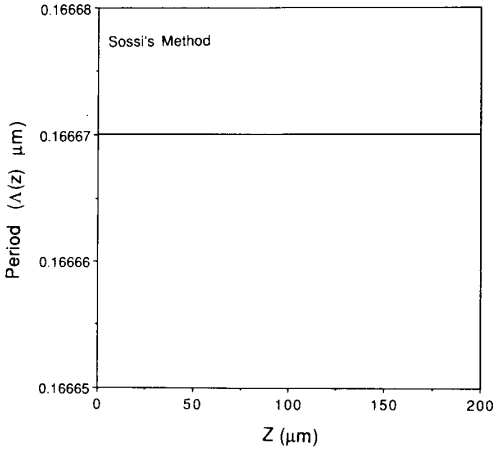

Fig. 7. Effective index period profile for the parabolic CWG filter.

paper indicates, however, that it's the optical thickness of a corrugation cycle, as opposed to its physical thickness, $\Lambda(z)$, which is the important quantity. The optical thickness, $OT(z)$, is defined as the average effective index of a cycle times its physical thickness. For effective index variations of the form given by (4.4), the average effective index N_0 is constant. Thus, $OT(z)$ is controlled solely through $\Lambda(z)$ as indicated by the equation below:

$$OT(z) = N_0\Lambda(z). \tag{5.2}$$

In practice, however, the waveguide corrugation is fabricated by etching into the top surface of the guiding layer through a metal patterning mask. As a result, one half of each corrugation cycle has the uncorrugated film/coverplate interface as its upper boundary. Thus, if the corrugation depth is not constant in z, then the average effective index is also a function of z. In this case, the effective index and the optical thickness profiles are given by

$$N_{\text{eff}}(z) = N_{\text{av}}(z) + \delta N_{\text{eff}}(z)$$
$$OT(z) = N_{\text{av}}(z)\,\Lambda(z). \tag{5.3}$$

The implications of (5.3) and (5.4) are mixed as far as fabrication is concerned. On the positive side they allow the required optical thickness profile to be easily realized through control of the corrugation depth, while maintaining a fixed physical thickness for each corrugation cycle. This point is important, because the required optical thickness variations are simply too small to be realized through changes in physical thickness alone (see Fig. 5). On the negative side, the corrugation depth profile affects both $\delta N_{\text{eff}}(z)$ and optical thickness simultaneously. Thus, these two parameters cannot be controlled independently. The fabrication of almost-periodic waveguide filters may require a several step process. First, the physical height of the uncorrugated guiding layer is slowly tapered. This tapering can be accomplished by etching the waveguide surface through a computer controlled movable slit. Second, a metal submicron periodic mask is created on the surface of the waveguide using holographic exposure techniques on photoresist, followed by metal evaporation. Finally, the periodic pattern is etched into the guiding layer, with an etch depth which depends on position z. This z dependence can be realized using either the slit approach discussed above or focused ion beam etching. By choosing the waveguide taper function and the etch (depth) profile properly, $\delta N_{\text{eff}}(z)$ and $OT(z)$ can be controlled separately as needed.

VI. Comparison with Other Design Techniques

In this section, our design results are compared with those obtained using 1) the first Born approximation Fourier-transform method [(3.10) and (4.13)], 2) the nonlinear renormalization Fourier-transform method] (3.12) and (4.13)], and 3) the exact Gel'fand-Levitan-Marchenko technique for two-component scattering systems.

Figs. 8 and 9 show the results of a "linear" filter design based on the first Born approximation and the nonlinear renormalization Fourier-transform methods, respectively. The first Born approximation is known to be inaccurate when the reflection coefficient is large. Thus, as Fig. 8 indicates, the first Born approximation method compares unfavorably with Sossi's technique. Fig. 9 indicates, however, that nonlinear renormalization and Sossi's method yield results of comparable accuracy. This is not surprising, since the $f(k)$ functions given by (3.11) and (3.12) are nearly identical as Table I indicates. Finally, note that the nonlinear renormalization approach has the advantage of being able to include the phase of the reflection coefficient in the design process.

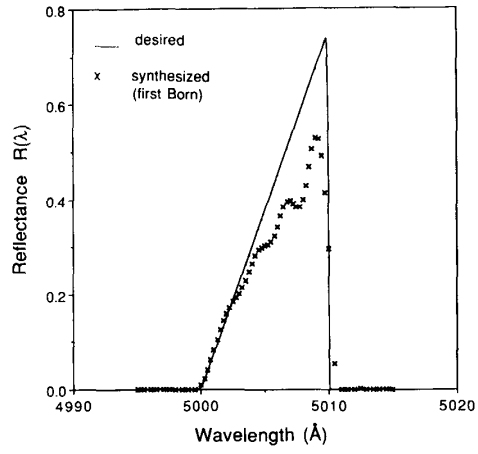

Fig. 8. Linear corrugated waveguide filter.

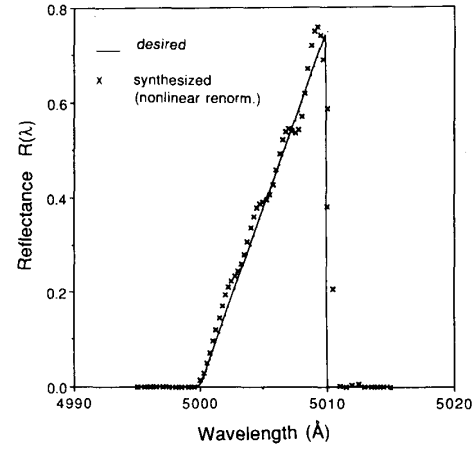

Fig. 9. Linear corrugated waveguide filter.

The Gel'fand-Levitan-Marchenko technique is an exact method for waveguide filter design. The detailed theory of this method can be found in [18] and [37] and will not be repeated here. In the following discussion we wish only to outline the general approach, indicate its complexity, and apply it to the design of the "linear" filter described in Section V.

Propagation through corrugated waveguide filters can be modeled by the following pair of coupled-mode equa-

TABLE I
ACCURACY OF THE APPROXIMATION $\tanh^{-1}[r] \approx [0.5(1/T - T)]^{1/2}$

r	$\tanh^{-1}(r)$	$[0.5(1/T - T)]^{1/2}$
0	0	0
0.100	0.100	0.100
0.200	0.203	0.202
0.300	0.309	0.307
0.400	0.423	0.423
0.500	0.549	0.540
0.600	0.692	0.679
0.700	0.866	0.852
0.800	1.095	1.099
0.900	1.467	1.593
1.000	∞	∞

tions [25]:

$$\frac{dB(z)}{dz} + i\delta(\lambda)\,B(z) = q(z)\,A(z) \tag{6.1}$$

$$\frac{dA(z)}{dz} - i\delta(\lambda)\,A(z) = q^*(z)\,B(z) \tag{6.2}$$

where $B(z)$ is the electric field amplitudes of the forward-propagating mode. $A(z)$ represents the electric field amplitude of the backward-propagating mode. $\beta(\lambda)$ is the propagating constant of the mode in the uncorrugated guide. $\delta(\lambda) = \beta(\lambda_0) - \beta(\lambda)$, where λ_0 is some fixed reference wavelength lying within the bandwidth of the filter, and $q(z) = a(z)\,e^{i\gamma(z)}$ is the coupling coefficient of the corrugation.

The filter design problem reduces to determining $q(z)$ given the reflection coefficient $A(0)/B(0)$ depending upon δ. When the reflection coefficient $r(\delta)$ can be written as a rational function of δ (and when several other conditions described in [18] are satisfied) it is possible to determine $q(z)$ exactly by solving sets of simultaneous linear equations [18]. The procedure is as follows. First, let $u = -i\delta$ and express $r(u)$ as a rational function $G(u) = P(u)/Q(u)$ where $Q(u)$ is a polynomial of order N and $P(u)$ is a polynomial of order $N - 1$ or less. Second, find the N roots of $Q(u)$ in the complex plane and denote them by $\rho_1, \rho_2, \cdots, \rho_N$. Third, form the polynomial $F(u) = Q(u)\,Q^*(-u^*) - P(u)\,P^*(-u^*)$, and find the $2N$ roots of $P(u)$ in the complex plane. Denote these roots by $\kappa_1, \kappa_2, \cdots, \kappa_N; \kappa_1^*, -\kappa_2^*, \cdots, -\kappa_N^*$. Fourth, solve the following system of $2N$ simultaneous linear equations

$$\sum_{m=1}^{N} \left\{ \frac{1}{G(\kappa_m)} \frac{\exp(-\kappa_m z)}{\rho_n - \kappa_m} \begin{bmatrix} d_{1,m}(z) \\ d_{2,m}(z) \end{bmatrix} - \frac{\exp(\kappa_m^* z)}{\rho_n + \kappa_m^*} \begin{bmatrix} d_{2,m}^*(z) \\ d_{1,m}^*(z) \end{bmatrix} \right\} = \begin{bmatrix} 1 \\ 0 \end{bmatrix}$$

$$\text{where } n = 1, \cdots, N \tag{6.3}$$

for values of z measured along the corrugated waveguide structure. Fifth, compute the coupling coefficient using (6.4) below.

$$q(z) = 2\sum_{n=1}^{N} d_{1,n}(z)\exp(\kappa_n z) - G(-\kappa_n^*)\,d_{2,n}^*(z)\exp(-\kappa_n^* z). \tag{6.4}$$

We have applied the above GLM technique to the "linear" filter described in Section V. We start by observing that

$$\delta(\lambda) \approx -\left[\frac{d\delta(\lambda)}{d\lambda}\right]_{\lambda=\lambda_0}(\lambda - \lambda_0) \tag{6.5}$$

$$= \frac{2\pi}{\lambda_0^2} N(\lambda_0)(\lambda - \lambda_0) - \frac{2\pi}{\lambda_0}\left[\frac{dN(\lambda)}{d\lambda}\right]_{\lambda=\lambda_0}(\lambda - \lambda_0) \tag{6.6}$$

$$\approx \frac{2\pi}{\lambda_0^2} N(\lambda_0)(\lambda - \lambda_0) \tag{6.7}$$

where $N(\lambda)$ is the effective index of the uncorrugated waveguide at wavelength λ. In our design we choose $\lambda_0 = 0.5005\ \mu$m, $N(\lambda_0) = 1.5$, and used (6.7) to determine $\delta(\lambda)$. The reflection coefficient of the filter was defined by

$$r(\lambda) = \begin{cases} [350(\lambda - 0.5000) + 0.35]^{1/2} & \\ \qquad 0.5000\ \mu\text{m} \le \lambda < 0.5010\ \mu\text{m} & \\ 0 \quad \text{elsewhere.} & \end{cases} \tag{6.8}$$

A fifth order, polynomial, least squares fit to $r(\delta)$ was performed over the wavelength range between 0.5000 and 0.5010 μm (i.e., $-0.01883 \le \delta \le 0.01883$). The result is

$$r(\delta) \approx P(\delta) = 9.354e07\delta^5 - 1.342e06\delta^4 - 1.8839e04\delta^3 + 19.168\delta^2 + 17.598\delta + 0.60691. \tag{6.9}$$

The denominator function $Q(\delta)$ was chosen to be a sixth order Butterworth filter with cut-off at $\delta = 0.01883$. This Butterworth filter effectively drives $G(\lambda)$ to zero for wavelengths lying outside the region between 0.5000 to 0.5010 μm. Fig. 10 shows a plot of the desired corrugated waveguide filter reflectance $|r(\lambda)|^2$ and the corresponding rational approximation $P(\lambda)/Q(\lambda)$ described above.

The coupling coefficient $q(z)$ was computed using (6.3) and (6.4) for z sampled every 1.5 μm, up to a total filter length of 750 μm. This calculation took approximately 10 minutes to complete on a MacIIx personal computer. The filter reflection coefficient was then reconstructed by numerically integrating the pair of coupled-mode equations (6.1) and (6.2). The reconstructed result is shown in Fig. 10, and is nearly identical to the rational reflection coefficient fit. Since the GLM technique is exact, the fit would have been perfect had the length of the filter not been truncated. Figs. 11 and 12 show the amplitude, $\delta N_{\text{eff}}(z)$ and the period $\Lambda(z)$ of the waveguide filter corresponding

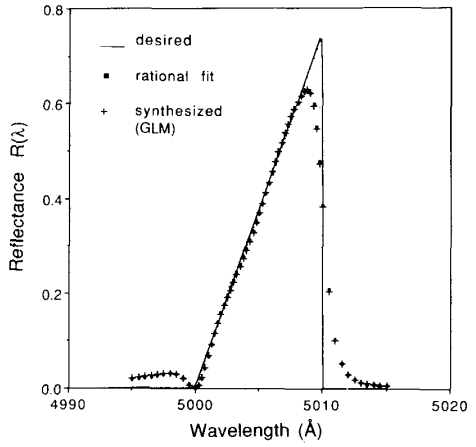

Fig. 10. Linear corrugated waveguide filter.

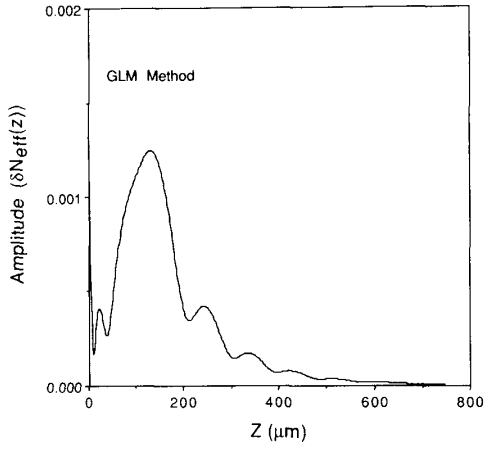

Fig. 11. Effective index amplitude profile for the linear CWG filter.

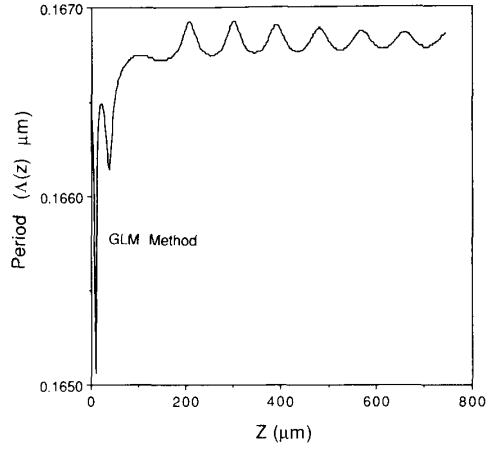

Fig. 12. Effective index period profile for the linear CWG filter.

to the coupling coefficient $q(z)$. The plots were generated using the following relationships [25].

$$N(z) = N_0 + \delta N_{\text{eff}}(z) \cos\left(\frac{2\pi}{\lambda} 2N_0 z + \gamma(z)\right) \tag{6.10}$$

$$\Lambda(z) = \frac{1}{\dfrac{2N_0}{\lambda_0} + \dfrac{1}{2\pi}\dfrac{d\gamma(z)}{dz}} \tag{6.11}$$

$$\delta N_{\text{eff}}(z) \approx N_0 a(z)\, \Lambda(z)/2 \tag{6.12}$$

with $\lambda_0 = 0.5005$ μm and $N_0 = 1.5$.

Note that the GLM technique described above is not truly exact, since its accuracy is limited by the rational polynomial fit to the reflection coefficient. Of course, the fit error can be made arbitrarily small, but only at the expense of increasing the number of design computations. As N gets large, numerical problems may also occur. For the examples studied in this paper, the GLM technique performed no better than the simpler Fourier-transform method.

VII. Conclusion

Coupling between forward- and backward-propagating modes of a thin film waveguide can be accomplished by corrugating the surface of the guide. The strength of the coupling interaction is a function of both the wavelength λ and the surface corrugation. The reflection coefficient $r(\lambda)$ defined as the ratio of the complex amplitudes of the backward to the forward-propagating guided modes, specifies the filter. The goal of corrugated waveguide filter design is to determine the needed surface corrugation given an $r(\lambda)$. The resulting corrugation is generally nonperiodic.

In this paper a new filter design technique has been developed for surface-corrugated waveguides. The technique is based on one-dimensional, Fourier-transform methods of inverse scattering theory and the effective index method for waveguide propagation. The approach is a direct extension of inverse scattering techniques previously applied to one-dimensional, dispersionless, dielectric media. The design method places only minor restrictions on the desired filter response. Furthermore, the design procedure is computationally fast, easy to implement, and numerically stable. The procedure is illustrated with two design examples. One of these designs has a parabolically-shaped reflectivity response $|r(\lambda)|^2$ while the response shape of the other design is linear. In both cases, good results are obtained.

The design of surface corrugated waveguide filters may also be performed using the Gel'fand-Levitan-Marchenko inverse scattering method for two component systems. In principle, this design method is exact when the reflection coefficient is in the form of a rational polynomial func-

tion. Since this condition is usually not satisfied, the GLM technique is inexact in practice. The accuracy of the technique is no better than one's ability to fit a rational polynomial function to the reflection coefficient data. Furthermore, this fit can only be improved by increasing the degree of the polynomials, which in turn, increases the number of computations required to perform the design. The examples considered in this paper indicate that the simpler Fourier-transform method can often produce adequate designs with much less computations.

Appendix

In this appendix, (2.23) and (2.24) of Section II are derived. These two equations relate the incremental change in waveguide effective index to an incremental change in either wavelength or corrugation height.

The derivation of (2.24) begins with the dispersion relationship, given below, for the TE modes of a waveguide [25]

$$V[1-b]^{1/2} = \tan^{-1}\left[b/(1-b)\right]^{1/2} + \tan^{-1}\left[(b+a)/(1-b)\right]^{1/2} \quad \text{(A.1)}$$

where

$$V(z) = \frac{2\pi}{\lambda} h(z)\left[n_f^2 - n_s^2\right]^{1/2} \quad \text{(A.2)}$$

$$N_{\text{eff}}(z) = \beta(z)\,(2\pi/\lambda)^{-1} \quad \text{(A.3)}$$

$$b(z) = \left(N_{\text{eff}}^2(z) - n_s^2\right)/\left(n_f^2 - n_s^2\right) \quad \text{(A.4)}$$

$$a = \left(n_s^2 - n_c^2\right)/\left(n_f^2 - n_s^2\right). \quad \text{(A.5)}$$

Differentiating both sides of (A.1) with respect to h yields

$$\frac{dV}{dh}[1-b]^{1/2} - \frac{1}{2}V\frac{db}{dh}\frac{1}{[1-b]^{1/2}} = \frac{1}{1+\frac{b+a}{1-b}}\frac{1}{2}\left(\frac{1-b}{b+a}\right)^{1/2}\frac{(1-b)+(b+a)}{(1-b)^2}\frac{db}{dh} + \frac{1}{1+\frac{b}{1-b}}\frac{1}{2}\left(\frac{1-b}{b}\right)^{1/2}\frac{(1-b)+b}{(1-b)^2}\frac{db}{dh} = \frac{1}{2}\frac{1}{[1-b]^{1/2}}\left(\frac{1}{b^{1/2}} + \frac{1}{(b+a)^{1/2}}\right)\frac{db}{dh}. \quad \text{(A.6)}$$

It follows from (A.2)-(A.4) that

$$\frac{dV}{dh} = \frac{2\pi}{\lambda}\left[n_f^2 - n_s^2\right]^{1/2} \quad \text{(A.7)}$$

$$\frac{dN_{\text{eff}}}{db} = \frac{\left(n_f^2 - n_s^2\right)}{2N_{\text{eff}}} \quad \text{(A.8)}$$

$$1 - b = \frac{n_f^2 - N_{\text{eff}}^2}{n_f^2 - n_s^2}. \quad \text{(A.9)}$$

Multiplying both sides of (A.6) by $[1-b]^{1/2}\,(dh)\,(dN_{\text{eff}}/db)$ and then using (A.7)-(A.9) yields

$$\frac{n_f^2 - N_{\text{eff}}^2}{N_{\text{eff}}}\,dh = \frac{\left(V + b^{-1/2} + (b+a)^{-1/2}\right)}{\frac{2\pi}{\lambda}\left[n_f^2 - n_s^2\right]^{1/2}}\,dN_{\text{eff}}. \quad \text{(A.10)}$$

It now follows from (A.10) that

$$\frac{dN_{\text{eff}}(z)}{N_{\text{eff}}(z)} = \frac{n_f^2 - N_{\text{eff}}^2(z)}{N_{\text{eff}}^2}\frac{dh(z)}{h_{\text{eff}}(z)} \quad \text{(A.11)}$$

where the effective waveguide height $h_{\text{eff}}(z)$ is given by [25]

$$h_{\text{eff}}(z) = \frac{\left(V + b^{-1/2} + (b+a)^{-1/2}\right)}{\frac{2\pi}{\lambda}\left[n_f^2 - n_s^2\right]^{1/2}}. \quad \text{(A.12)}$$

This establishes the desired result since (2.24) and (A.11) are identical.

The derivation of (2.23) proceeds in a similar manner. The dispersion relationship (A.1) is differentiated with respect to λ to yield

$$-\frac{1}{\lambda}V[1-b]^{1/2} - \frac{1}{2}V\frac{db}{d\lambda}\frac{1}{[1-b]^{1/2}} = \frac{1}{2}\frac{1}{[1-b]^{1/2}}\left(b^{-1/2} + (b+a)^{-1/2}\right)\frac{db}{d\lambda}. \quad \text{(A.13)}$$

Multiplying both sides of (A.13) by $[1-b]^{1/2}\,(dN_{\text{eff}}/db)$, and then using (A.8), (A.9), and (A.12) produces the desired result

$$\frac{dN_{\text{eff}}(z)}{N_{\text{eff}}(z)} = \frac{-h(z)}{h_{\text{eff}}(z)}\frac{\left(n_f^2 - N_{\text{eff}}^2(z)\right)}{N_{\text{eff}}^2(z)}\frac{d\lambda}{\lambda}. \quad \text{(A.14)}$$

References

[1] A. Yariv and M. Nakamaura, "Periodic structures for integrated optics," *IEEE J. Quantum Electron.*, vol. QE-13, pp. 233-253, Apr. 1977.

[2] H. Kogelnik and C. V. Shank, "Coupled wave theory of distributed feedback lasers," *J. Appl. Phys.*, vol. 43, pp. 2327-2335, May 1972.

[3] G. I. Stegeman and C. J. Seaton, "Nonlinear integrated optics," *J. Appl. Phys.*, vol. 58, pp. R57-R78, Dec. 1985.

[4] S. Somekh and A. Yariv, "Phase-matchable nonlinear interactions in periodic thin films," *Appl. Phys. Lett.*, vol. 21, pp. 140-141, Aug. 1972.

[5] B. U. Chen, C. C. Ghizoni, and C. L. Tang, "Phase-matched second harmonic generation in solid thin films using modulation of the nonlinear susceptibilities," *Appl. Phys. Lett.*, vol. 28, pp. 651-653, June 1976.

[6] J. P. van der Ziel, M. Llegems, D. W. Foy, and R. M. Mikulyak, "Phase-matched second harmonic generation in a periodic GaAs waveguide," *Appl. Phys. Lett.*, vol. 29, pp. 775-777, Dec. 1976.

[7] M. L. Dakss, L. Kuhn, P. F. Heidrich, and B. A. Scott, "Grating coupler for efficient excitation of optical guided waves in thin films," *Appl. Phys. Lett.*, vol. 16, pp. 523-525, June 1970.

[8] D. C. Flanders, H. Kogelnik, R. V. Schmidt, and C. V. Shank, "Grating filters for thin-film optical waveguides," *Appl. Phys. Lett.*, vol. 24, pp. 194-196, Feb. 1974.

[9] K. O. Hill, "Aperiodic distributed-parameter waveguides for integrated optics," *Appl. Opt.*, vol. 13, pp. 1853-1956, Aug. 1974.
[10] R. V. Schmidt, D. C. Flanders, C. V. Shank, and R. D. Standley, "Narrow-band grating filters for thin-film optical waveguides," *Appl. Phys. Lett.*, vol. 25, pp. 651-652, Dec. 1974.
[11] H. Kogelnik, "Filter response of nonuniform almost-periodic structures," *Bell System Tech. J.*, vol. 55, pp. 109-126, Jan. 1976.
[12] C. S. Hong, J. B. Shellan, A. C. Livanos, A. Yariv, and A. Katzir, "Broad-band grating filters for thin-film optical waveguides," *Appl. Phys. Lett.*, vol. 31, pp. 276-278, Aug. 1977.
[13] J. B. Shellan, C. S. Hong, and A. Yariv, "Theory of chirped gratings in broad band filters," *Opt. Commun.*, vol. 23, pp. 398-400, Dec. 1977.
[14] S.-H. Kim and C. G. Fonstad, "Tunable narrow-band thin-film waveguide grating filters," *IEEE J. Quantum Electron.*, vol. QE-15, pp. 1405-1408, 1979.
[15] H. J. Lee, N. A. Olsson, C. H. Henry, R. F. Kazarinov, and K. J. Orlowsky, "Narrowband Bragg reflector filter at 1.52 μm," *Appl. Opt.*, vol. 27, pp. 211-213, Jan. 1988.
[16] M. Matsuhara and K. O. Hill, "Optical-waveguide band-rejection filters: Design," *Appl. Opt.*, vol. 13, pp. 2886-2888, Dec. 1974.
[17] M. Matsuhara, K. O. Hill, and A. Watanabe, "Optical-waveguide filters: Synthesis," *J. Opt. Soc. Amer.*, vol. 65, pp. 804-808, July 1975.
[18] G.-H. Song and Sang-Yung Shin, "Design of corrugated waveguide filters by the Gel'Fand Levitan-Marchenko inverse-scattering method," *J. Opt. Soc. Amer.*, vol. 2, pp. 1905-1915, Nov. 1985.
[19] E. Delano, "Synthesis of multilayer filters," *J. Opt. Soc. Amer.*, vol. 57, pp. 1529-1533, Dec. 1967.
[20] L. Sossi, "A method for synthesis of multilayer dielectric interference coatings," *Eesti NSV Teaduste Akadeemia Toimetised Fuusika Matemaatika*, vol. 25, pp. 229-237, 1974. (Translations of [20]-[24] are available from the Translation Services of the Canada Institute for Scientific and Technical Information, National Research Council of Canada, Ottawa, Ontario, Canada K1A 0R6).
[21] L. Sossi and P. Kard, "On the theory of the reflection and transmission of light by a thin inhomogeneous dielectric film," *Eesti NSV Teaduste Akadeemia Toimetised Fuusika Matemaatika*, vol. 17, pp. 41-48, 1968.
[22] L. Sossi, "On the theory of the synthesis of multilayer dielectric light filters," *Eesti NSV Teaduste Akadeemia Toimetised Fuusika Matemaatika*, vol. 25, pp. 171-176, 1976.
[23] ——, "On the synthesis of interference coatings," *Eesti NSV Teaduste Akadeemia Toimetised Fuusika Matemaatika*, vol. 26, N-1.1., 1977.
[24] ——, "Synthesis of dielectric interference filters with narrow reflection bands," *Eesti NSV Teaduste Akadeemia Toimetised Fuusika Matemaatika*, vol. 28, pp. 213-220, 1979.
[25] H. Kogelnik, "Theory of dielectric waveguides," in *Integrated Optics*, T. Tamir, Ed. New York: Springer-Verlag, 1979.
[26] K. Chadan and P. C. Sabatier, *Inverse Problems in Quantum Scattering Theory*. New York: Springer-Verlag, 1977.
[27] J. A. Dobrowolski and D. Lowe, "Optical thin film synthesis program based on the use of Fourier transforms," *Appl. Opt.*, vol. 17, pp. 3039-3050, Oct. 1978.
[28] ——, "Comparison of the Fourier transform and flip-flop thin-film synthesis methods," *Appl. Opt.*, vol. 25, pp. 1966-1972, June 1986.
[29] P. G. Verly, J. A. Dobrowolski, W. J. Wild, and R. L. Burton, "Synthesis of high rejection filters with the Fourier transform method," *Appl. Opt.*, vol. 28, pp. 2864-2875, July 1989.
[30] G. Boivin and D. St. Germain, "Synthesis of gradient-index profiles corresponding to spectral reflectance derived by inverse Fourier transform," *Appl. Opt.*, vol. 26, pp. 4209-4213, Oct. 1987.
[31] D. L. Jaggard and Y. Kim, "Accurate one-dimensional inverse scattering using a nonlinear renormalization technique," *J. Opt. Soc. Amer. A*, vol. 2, pp. 1922-1930, Nov. 1985.
[32] A. Basu and J. M. Ballantyne, "Random fluctuations in first order waveguide grating filters," *Appl. Opt.*, vol. 18, pp. 2575-2579, Aug. 1979.
[33] P. Verly, R. Tremblay, and J. W. Y. Lit, "Application of the effective index method to the study of distributed feedback in corrugated waveguides. TE polarization," *J. Opt. Soc. Amer.*, vol. 70, pp. 964-968, Aug. 1980.
[34] K. A. Winick, "The effective index method and coupled mode theory for almost-periodic waveguide gratings: A comparison," submitted to *Appl. Opt.*
[35] P. Verly, R. Tremblay, and J. W. Y. Lit, "Application of the effective index method to the study of distributed feedback in corrugated waveguides. TM polarization," *J. Opt. Soc. Amer.*, vol. 70, pp. 1218-1221, Oct. 1980.
[36] C. H. Greenewalt, W. Brandt, and D. D. Friel, "Irridescent colors of hummingbird feathers," *J. Opt. Soc. Amer.*, vol. 50, pp. 1005-1013, Oct. 1960. (See also ref. [11] given in [31] above.)
[37] G. L. Lamb, Jr., *Elements of Soliton Theory*. New York: Wiley, 1980.

Kim A. Winick (S'77-M'80) was born in New York, NY, on July 27, 1954. He received the B.S. degree in electrical engineering from the Pennsylvania State University, University Park, in 1976, and the M.S. and Ph.D. degrees in electrical engineering from the University of Michigan, Ann Arbor, in 1977 and 1981, respectively. While at the University of Michigan, he held a National Science Foundation Graduate Fellowship.

From 1981 until 1988, he was a technical staff member at the Lincoln Laboratory, Massachusetts Institute of Technology, working on millimeter wave and coherent optical communications systems. Since autumn of 1988, he has been an Assistant Professor in the Department of Electrical Engineering and Computer Science at the University of Michigan, Ann Arbor. His major research interests include optical communications systems and devices.

Dr. Winick is a member of the Optical Society of America.

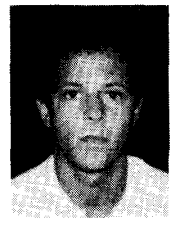

Jose E. Roman was born in San Juan, PR, in 1965. He received the B.S. degree in electrical engineering from the University of Florida, Gainesville, in 1987, and the M.S. degree from the University of Michigan, Ann Arbor, in 1989.

He is currently pursuing the Ph.D. degree in electrical engineering at the University of Michigan. His area of interest is integrated optics.

Mr. Roman is a member of the Optical Society of America.